How Do Self-Ordered Silver Nanocrystals Influence Their Growth into Triangular Single Crystals?

ARTICLE *in* THE JOURNAL OF PHYSICAL CHEMISTRY C · DECEMBER 2007

Impact Factor: 4.77 · DOI: 10.1021/jp076227z

4 AUTHORS, INCLUDING:

Anne-Isabelle Henry
Northwestern University
20 PUBLICATIONS **1,446** CITATIONS

SEE PROFILE

Nicolas Goubet
Pierre and Marie Curie University - Paris 6
28 PUBLICATIONS **552** CITATIONS

SEE PROFILE

How Do Self-Ordered Silver Nanocrystals Influence Their Growth into Triangular Single Crystals?

A.-I. Henry, A. Courty, N. Goubet, and M.-P. Pileni*

Laboratoire LM2N, CNRS, UMR 7070, Université P. et M. Curie (Paris VI), BP 52 4 place Jussieu, 75252 Paris Cedex 05, France

Received: August 3, 2007; In Final Form: September 24, 2007

Thin triangular silver single crystals are obtained by annealing self-ordered 5 nm silver nanocrystals coated with decanethiol at 50 °C and deposited on highly oriented pyrolitic graphite (HOPG). With the annealing time, the nanocrystals coalesce progressively in the 2D hexagonal arrays and 3D face-centered cubic (fcc) superlattices. By controlling the ordering degree of the nanocrystal assemblies, we observe that the size of the ordered domains tunes the final size of the triangles.

1. Introduction

During this last decade, numerous nanometer-sized materials have been ordered in 2D and 3D superlattices, resulting in the formation of fcc "supra" crystals. The first self-ordered nanocrystals were obtained simultaneously by our group[1] and that of Bawendi[2] by using semiconductors such as Ag_2S and CdSe. This was extended to other semiconductors, various metals, and metal oxides.

It has been discovered that the ordering of nanocrystals in 2D and small 3D superlattices induces collective physical properties mainly due to dipolar interactions induced by the high vicinity of the nanocrystals.[3] Furthermore, it has been demonstrated that the shape of the nanocrystal ordering induces change in the physical properties of the assemblies.[4−6]

In our group over the last few years, we have concentrated on exploring the influence of the nanocrystal ordering on the physical properties of such assemblies. As has been observed in nature, opal crystals show specific reflectivities due to the ordering of SiO_2 nanocrystals with a color dependence on the nanocrystal size, whereas milk-like crystals are observed when the nanocrystals are disordered.[7] Recently, we obtained evidence, by low-frequency Raman scattering, of intrinsic vibrational coherence in fcc supracrystals made of silver nanocrystals.[8,9] Similar collective properties are observed for 3D superlattices made of cobalt nanocrystals.[3,10] The nanocrystal superlattices can be thus referred to as artificial solids in which the nanocrystals behave as atoms in traditional solids. We have also shown intrinsic mechanic and magnetic properties of self-ordered cobalt nanocrystals.[11,12]

A lot of work carried out under ultrahigh vacuum (UHV) has been reported on the epitaxial growth of metal particles on substrates with a specific orientation.[13−21] Recently, triangular silver particles have been obtained by chemical reduction of metal salts[22,23] and photoinduced aggregation of small nanoparticle seeds.[24,25]

In the present paper, it is shown that a mild annealing (50 °C) of self-ordered 5 nm silver nanocrystals coated with decanethiols and deposited on highly oriented pyrolitic graphite (HOPG) induces the formation of epitaxially oriented large triangular silver single crystals (several tens of nanometers).

2. Experimental Section

2.1. Apparatus. Transmission electron microscopy (TEM), high-resolution electron microscopy (HRTEM), and scanning electron microscopy (SEM) images were obtained with JEOL JEM 1011, JEOL JEM 2010, and JEOL JSM-5510LV instruments, respectively. Small-angle X-ray diffraction (SAXD) was performed with a homemade system with a copper anode.[8,9]

2.2. Synthesis of Silver Nanocrystals. Silver nanocrystals are synthesized in functionalized mixed reverse micelles, as described previously.[26] Silver nanocrystals are obtained by mixing two reverse micellar solutions. The first is made of 60% 0.1 M functionalized surfactant Ag(AOT) (silver di(2-ethylhexyl) sulfosuccinate) and 40% 0.1 M Na(AOT) dissolved in isooctane. The water content $w = [H_2O]/[AOT]$ is kept at 2. The second solution is 0.1 M Na(AOT) in isooctane, with water replaced by hydrazine. Hydrazine is in excess, and its content, defined as $R = [N_2H_4]/[AOT]$, is kept at 1.44. The silver ion reduction starts as soon as the two solutions are mixed and is stopped several hours later by the addition of decanethiols in the solution (3 μL/mL). The remaining surfactant is removed by ethanol addition, inducing flocculation of the decanethiol-coated (C10-Ag) nanocrystals. This precipitate is then dispersed in hexane. In order to reduce the size distribution, a size-selective precipitation process[26] is carried out by progressively adding pyridine to the colloidal solution. An agglomeration of the largest particles takes place, which allows them to be collected in a precipitate after centrifugation. The latter is then dispersed in decane, leading to a homogeneous clear solution of nanocrystals. Silver nanocrystals are characterized by a mean diameter of 5.0 nm and a size distribution of 12%. A mixture of cubooctahedral, decahedral, and icosahedral nanocrystals is produced.[27]

2.3. Sample Preparation. The preparation of the samples differs slightly when the analysis of the samples is performed by TEM or SEM and small-angle X-ray diffraction. In all the cases, the substrate (HOPG) is immersed in a silver nanocrystal colloidal solution. The samples are put in an oven (50 °C) for either 20 h (corresponding to the evaporation time of decane)

* To whom correspondence should be addressed. E-mail: pileni@sri.jussieu.fr.

10.1021/jp076227z CCC: $40.75
Published on Web 12/12/2007

or 8 days. The concentration ([Ag]= 1.6×10^{11} nanocrystals/μL), temperature (50 °C), and solvent (decane) remain unchanged.

The TEM grid (diameter 3 mm), covered by HOPG, is immersed in 50 μL of the colloidal solution. For the SEM and X-ray diffraction measurements, the HOPG solid substrate (5 mm x 5 mm) is immersed in a higher volume (200 μL) of the colloidal solution. According to the different sizes of the substrates, different sized vessels are used. Nevertheless, the deposited volume of colloidal solution has been chosen in order to maintain the number of nanocrystals per surface unit constant. Nevertheless, in some cases, as noted in the text, the experimental conditions (volume and nanocrystal concentration) slightly change.

3. Results and Discussion

By deposition of the C10-Ag solution as described in the Experimental Section, the nanocrystals self-assemble at long range in 2D and in 3D (Figure 1A and B). The small angle electron diffraction (SAED) patterns (inset Figure 1B) corresponding to the 3D assemblies indicate a sixfold symmetry, suggesting that the nanocrystal arrangement normal is [111] if we consider a fcc packing, which will be confirmed by SAXD (see below). By deposition of 200 μL instead of 50 μL of colloidal solution on HOPG (5 mm $\times$ 5 mm), large nanocrystal assemblies looking like pavements with an average height of 1 μm and an average surface area of several hundreds of micrometers are observed by SEM (Figure 1C and inset). The corresponding diffraction pattern (Figure 1D) presents two well-defined Bragg reflections normal to the substrate and four pairs of diffraction spots characteristic of a fcc packing. A very good agreement between the observed and calculated diffraction spot coordinates for fcc packing is observed (Table 1). The reflection width (HWHM = 0.05 nm^{-1}) is nearly resolution-limited, indicating long-range ordering of the silver particles perpendicular to the surface. From the stacking periodicity ($D\sqrt{2/3} = 5.60 \pm 0.05$ nm), the particle coated diameter (D) is equal to 6.90 nm, which is close to the value determined by SAED. According to the core diameter of nanocrystals deduced from TEM (5.0 nm), we calculate a coating contribution of 1.90 nm, implying a partial interdigitation of the C10 chains (80%), which have a length of 1.52 nm in a cis−trans configuration.[28]

After annealing for 8 days the sample described in Figure 1A and B and characterized by mono- and multilayers of highly ordered nanocrystals, the TEM images show large equilateral triangular-shaped particles (Figure 2A and B), which are flat and more or less truncated at the edges. These triangular particles represent 29% of the total number of coalesced particles with a diameter larger than 5 nm. The triangle size (defined as the diameter of the circle surrounding each particle) is between 15 and 940 nm. Several triangles are aligned on the substrate (see dotted lines in Figure 2A). Some of them are very close, and their edges are parallel (Figure 2B). Other various shapes are also observed among all of the coalesced particles; 6% of them are decahedral particles with a pentagonal profile of maximum size around 200 nm (Figure 2C), 3% are hexangular particles with more or less rounded edges (Figure 2D), 19% are characterized by pieces of triangles or hexagons, and 43% correspond to ill-defined particles. In some cases, large faceted particles are superimposed on a triangular particle (Figures 2A and 3A). The dark-field TEM image (Figure 3B) shows a very bright faceted triangular particle, indicating a strongly diffracting crystal and consequently well-crystallized object. We observe also that the superimposed particles are illuminated, whereas the overall particles are not. The HRTEM images obtained for this part of the superimposed particles (Figure 3C and 3D) show that the lattice fringes of both particles are not aligned, and consequently, no crystalline relationship exists between them. Sometimes, Moiré fringes appear, indicating that the misorientation of the lattice plane is small. Hence, the partial illumination of the superimposed particles is mainly due to the fact that they are very thin and illuminated through the triangular single crystals. The superimposed thin flat particles have been formed independently in the 3D superlattices by a layer by layer nanocrystal coalescence.

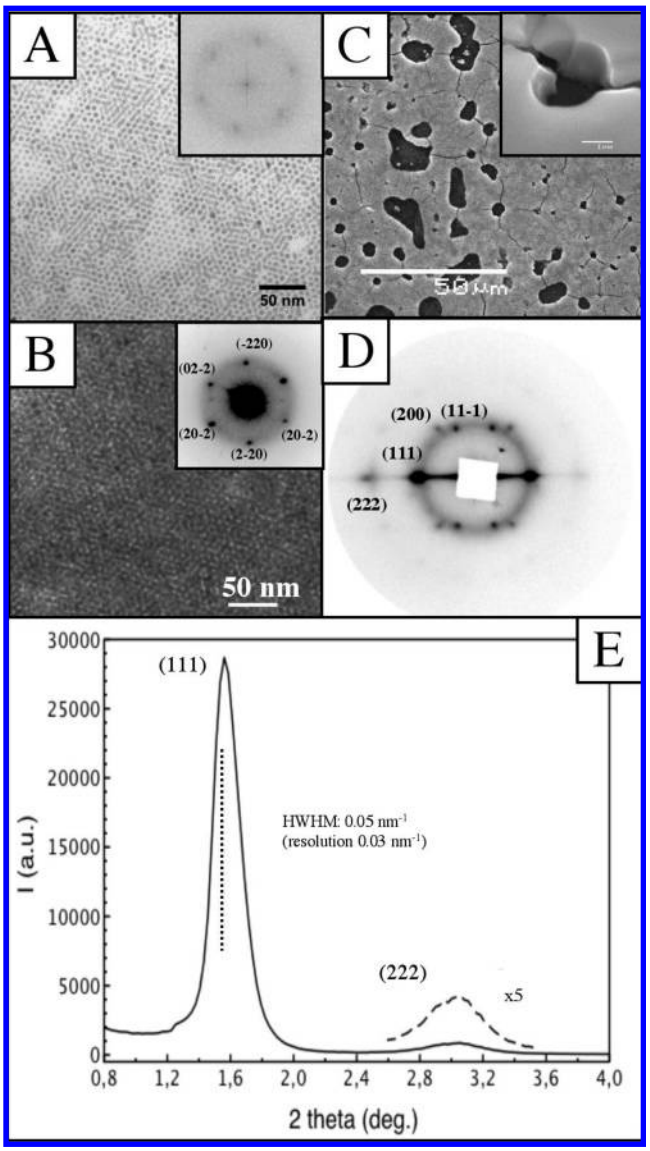

Figure 1. Silver nanocrystal organizations after 20 h of annealing at 50 °C. (A) TEM image of a 2D assembly and corresponding PS in the inset. (B) TEM image of a 3D assembly and corresponding SAED pattern in the inset. (C) SEM image of a 3D assembly and higher magnification (tilted by 30°) in the inset. (D) SAXD pattern of a 3D assembly. (E) Profile of the diffraction pattern along the (111) and (222) Bragg reflections.

TABLE 1: 3D Deposition of Silver Nanocrystals on HOPG; Comparison between Experimental and Calculated Coordinates of Diffraction Spots Assuming a fcc Structure[a]

[h k l] indices	q^x_{hkl} (meas.) $Å^{-1}$	q^x_{hkl} (calc.) $Å^{-1}$	q^y_{hkl} (meas.) $Å^{-1}$	q^y_{hkl} (calc.) $Å^{-1}$	d_{hkl} (meas.) nm	d_{hkl} (calc.) nm
1 1 −1	0.35	0.36	0.98	1.03	6.03	5.76
2 0 0	0.72	0.73	0.96	1.03	5.23	4.98
1 1 1	1.09	1.10	0	0	5.73	5.71
2 2 2	2.15	2.19	0.05	0	2.92	2.87

[a] See Figure 1D.

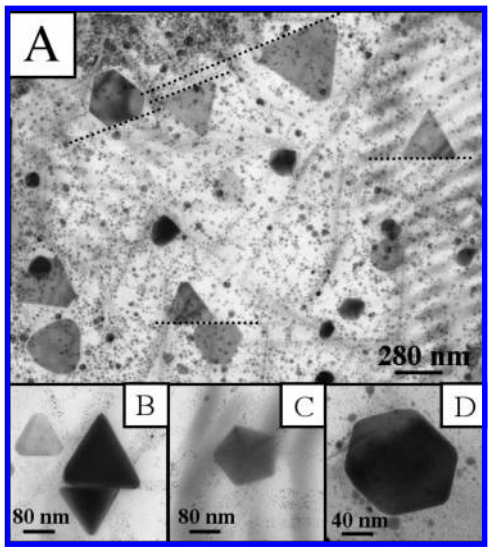

Figure 2. Silver nanocrystals obtained from self-assembled silver nanocrystals annealed for 8 days. (A) Typical TEM image at low magnification. The dotted lines show the alignment of the particles. (B−D) Nanocrystals with different shapes, (B) triangles, (C) decahedron, and (D) hexagonal particle.

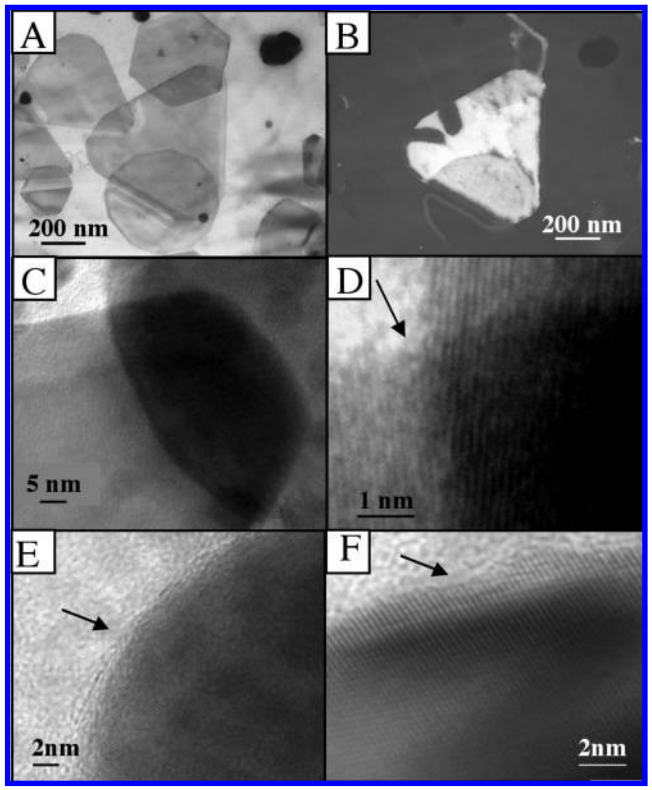

Figure 3. Superimposed triangular silver nanocrystals. (A and B) Bright- and dark-field TEM images, respectively, of superimposed particles. (C and D) HRTEM images of superimposed triangular particles. (E and F) HRTEM images performed on the edges of different triangular particles.

The HRTEM images obtained at the edges of the triangular single crystals show either a thin amorphous layer (see arrow in Figure 3E) or well-defined edges (see arrow in Figure 3F). The amorphous layer could be due either to the presence of thiol molecules which remain attached to the triangles, possibly observed in particular focus conditions,[29] or to a thin amorphous silver oxide layer as the experiment is carried out in air. However, in the latter case, we would expect to observe such

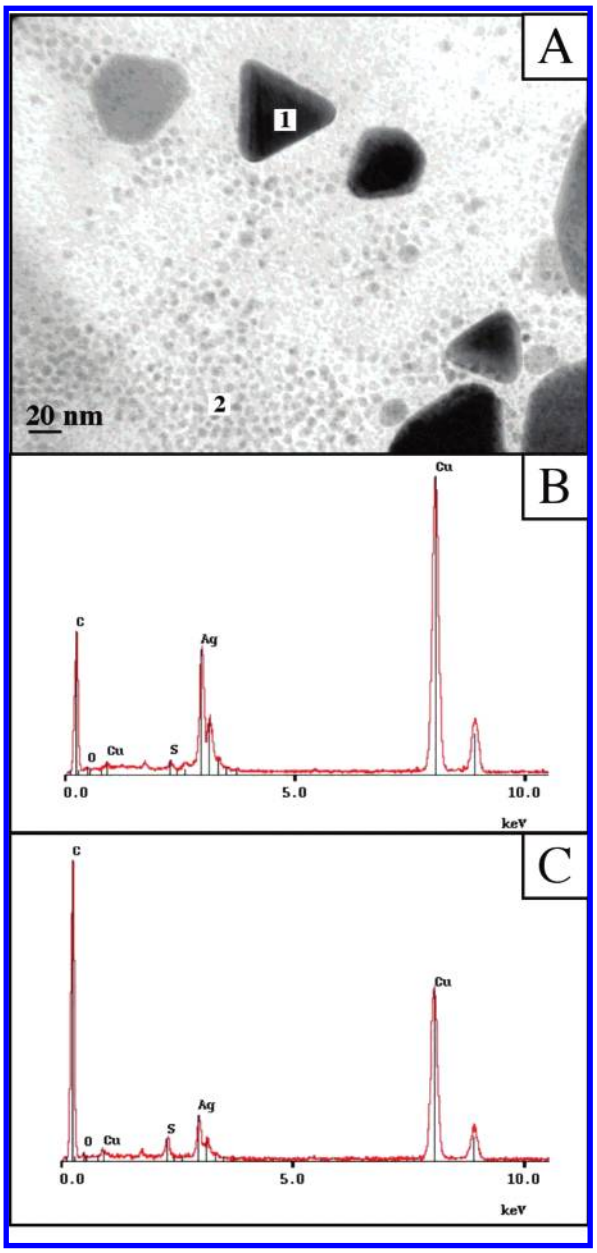

Figure 4. Detection of silver oxide by EDX measurements. (A) TEM image of 8 day annealed silver nanocrystals with different shapes and sizes. (B) EDX profile performed on the triangle numbered 1 in (A). (C) EDX profile performed on the area numbered 2 in (A).

an amorphous layer on all of the coalesced silver particles. Thus, if oxygen is present, it seems difficult to detect it by HRTEM. In order to establish the atomic composition of these particles, energy dispersive X-ray (EDX) measurements have been performed. The measurement performed on a triangle (numbered 1 in Figure 4A) shows a very small amount of oxygen ($I_O/I_{Ag} \leq 2\%$) and the presence of carbon and sulfur (Figure 4B). Similar measurements on an assembly of spherical nanoparticles (numbered 2 in Figure 4A) show, as on large triangular single crystals, a very small amount of oxygen ($I_O/I_{Ag} \leq 2\%$), sulfur, and carbon atoms (Figure 4C). Because of the presence of these last two components, it is clear that the triangular single silver particles are still capped by thiol alkyl chains. This could explain the high stability of the triangle regarding oxidation. A recent paper[30] shows that even under a beam containing hyperthermal atomic oxygen, bulk metal silver material loses its crystallinity with the formation of a thick amorphous layer of silver oxide

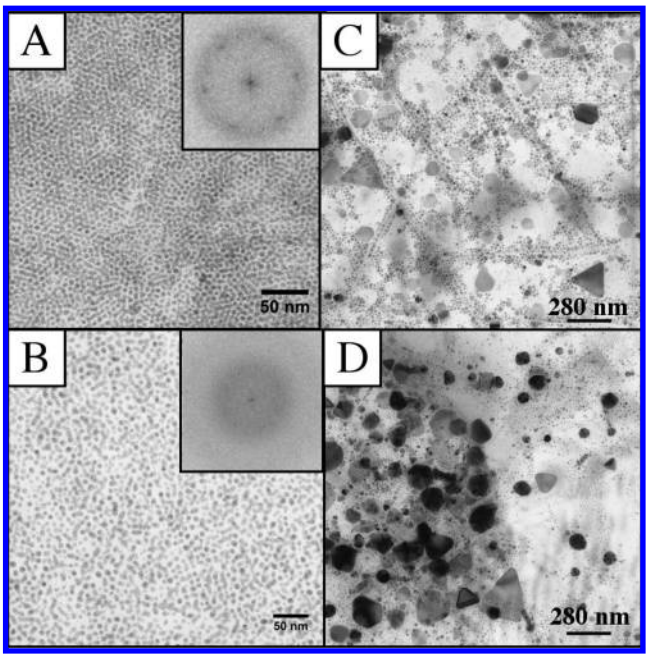

Figure 5. Effect of the nanocrystal ordered domain size on the triangle final size. (A and C) $V = 20\ \mu L$, $c = 1.6 \times 10^{11}$ nanocrystals/μL. (A) Silver nanocrystal organization after 20 h of annealing and the corresponding PS in the inset. (C) Particles obtained after 8 days of annealing. (B and D) $V = 20\ \mu L$, $c = 4.0 \times 10^{11}$ nanocrystals/μL. (B) Silver nanocrystal organization after 20 h of annealing and the corresponding PS in the inset. (D) Particles obtained after 8 days of annealing.

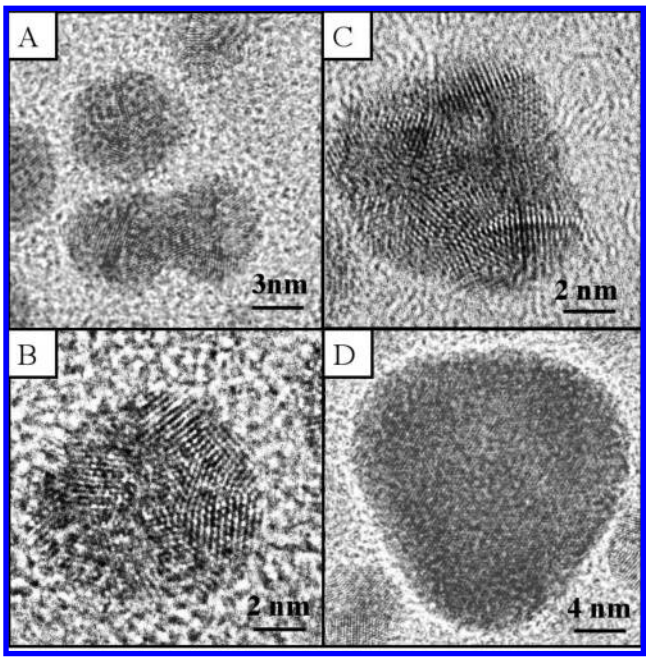

Figure 6. HRTEM performed on coalesced silver nanocrystals obtained after 6 days of annealing at 50 °C. (A) Neck formation between two twinned particles. (B and C) Coalesced particles with remaining structural stress (twin boundaries). (D) Newly formed triangular particle totally relaxed without structural defects.

containing only 3−5 atoms % of oxygen. The authors assume that this phenomenon is due to a thermal reduction of Ag_2O at 220 °C. In our experimental conditions, the amorphous layer is very thin, and a very small amount of oxygen, less than 2%, is measured. Nevertheless, the silver materials are not subjected to such a strong oxygen attack, and they are protected by a capping agent (decanethiols). These two conditions lead us to expect less oxygen damage. Note that the I_S/I_{Ag} for the triangular single crystals is 10 times smaller than that of the noncoalesced particles (Figure 4B and C). If we assume that the thiol coverage rate is constant, the increase of the volume/surface ratio for the triangles compared to the particles explains the decrease of the ratio I_S/I_{Ag}. Hence, the presence of a very small amount of silver oxide on silver triangular single crystals covered by thiol molecules cannot be excluded.

At the first stage of the triangle formation process, the silver nanocrystals are self-organized in 2D and 3D. For understanding of the triangle formation mechanism, it is important to know the role of the nanocrystal ordering. The high vicinity of the nanocrystals in the superlattices should favor their coalescence. To support such a claim, the silver nanocrystal ordering is slightly changed from compact to disordered ordering. In order to get disordered assemblies, the experimental conditions have been slightly changed (volume V used and concentration c of the initial C10-Ag solution in decane). As described above (Figure 1A), a compact ordering at large scale is obtained by slow evaporation of 50 μL of a colloidal solution characterized by a concentration of 1.6×10^{11} nanocrystals/μL. By decreasing the volume from 50 to 20 μL and keeping the same colloidal concentration (1.6×10^{11} nanocrystals/μL), Figure 5A shows a decrease in the ordering with diffuse spots on the corresponding PS (inset Figure 5A). A higher decrease in the ordering (Figure 5B) is observed by keeping the volume constant (20 μL) and by increasing the colloidal concentration to 4×10^{11} nanocrystals/μL. The diffuse ring on the corresponding PS (inset Figure 5B) confirms this disorder. For simplicity, let us call samples A, B, and C the three samples differing by the ordering of the nanocrystals and shown in Figures 1A, 5A, and 5B, respectively. Sample A has been largely described above with the formation under mild annealing of large, flat, thin fcc single crystals. After annealing sample B at 50 °C, rather large triangular crystals are observed (Figure 5C), with sizes almost five times lower than those observed in Figure 1A. The TEM images in the bright and dark (see Supporting Information Figure S1A and B, respectively) fields show that the flat triangular particles are thin and well-crystallized, as observed above. After annealing of sample C, the TEM images show a very large amount of nanocrystals with various shapes (Figure 5D). However, flat and thin triangular crystals are still present. As previously, the TEM in the bright and dark fields (see Supporting Information, Figure S1C and D, respectively) show that they are well-crystallized, with sizes 10 times smaller than those obtained for sample A. Hence, comparison between Figures 1A, 5A, and 5B allows one to conclude that initial nanocrystal range order tunes the final size of the triangles and that reducing the interparticle distance favors the nanocrystal coalescence. In a previous paper, the ordering range had been decreased by changing the substrate HOPG by amorphous carbon (keeping the same experimental conditions as those for sample A), and we had also observed a decrease in the final size of the triangles.[31] The data obtained in this paper allow thus to neglect the contribution of the roughness of the substrate in the control of the size of the triangles. Concerning the nanocrystal coalescence process, it is important to point out that the initial deposited nanocrystals start to coalesce only after 3 days of annealing.[31] After 6 days, we observe by TEM a mixture of noncoalesced and coalesced particles.[31] We have observed samples annealed for 6 days by HRTEM (Figure 6). Figure 6A−C shows partially coalesced twinned particles. Twin planes maintain their adhesion. Figure 6D shows totally relaxed triangular particles with rounded edges without structural

defects. This implies a complete atomic rearrangement and a removal of twin planes. The annealing process markedly increases the mobility of the alkyl chains on the substrate,[32] making the movement of the nanocrystals to their neighbors easier.

Although the substrate does not control the final size of the silver triangles, it plays a role in their mechanism of formation as, at the end of the process, we observe that they are epitaxially oriented. Indeed, electron diffraction has been performed on triangular particles (see ref 31 and Supporting Information, Figure S2). The patterns reveal that most of the triangles (70%) are in a same epitaxial orientation, which is defined by $(111)_{Ag}$//$(00.1)_{HOPG}$ and $[\bar{1}10]_{Ag}$//$[\bar{1}\bar{1}.0]_{HOPG}$. A second epitaxial orientation is also observed for 20% of the silver particles, which is defined by $(111)_{Ag}$//$(00.1)_{HOPG}$ and$[\bar{1}10]_{Ag}$//$[10.0]_{HOPG}$. The remaining 10% of triangles show no preferential orientation with HOPG.

The morphological (size and shape) evolution of the coalesced silver particles during the annealing time suggests that Ostwald ripening in two dimensions (2D) can also contribute to their growth.[33,34] Indeed, upon increasing the annealing time, the triangle size distribution evolves to consist of larger triangles. The larger triangles grow at the expense of smaller ones. Few triangles have rounded edges (Figure 2A and 6D) because the atoms located on the edges are weakly bounded. They can thus rapidly vanish, diffusing on the surface in order to transfer to a larger triangle. The 2D ripening is thus limited by surface diffusion and by attachment/detachment of atoms to the silver particle edges.[35] Nevertheless, that does not exclude the fusion of small triangles into larger ones, which could also explain the size evolution of the silver particles. This is consistent with Jin et al.,[24] who observe a light-induced fusion of nanoprisms in solution.

4. Conclusion

We report in this paper on the formation of triangular single crystals by heat-induced coalescence of self-ordered silver nanocrystals. By tuning the initial nanocrystal ordering on a same substrate (HOPG), we show that the final size of the triangles is controlled by the size of the ordered domains and not by the nature of the substrate. During the annealing, large triangular particles grow at the expense of the smaller ones via a coalescence process, which is favored by the high vicinity of the self-ordered nanocrystals.

Acknowledgment. Thanks are due to Pr. Jacob Israelachvili for fruitful discussions, to Dr. P. A. Albouy for the small-angle X-ray diffraction experiments, and also to Dr. D. Parker for checking the English in this paper.

Supporting Information Available: TEM images and electron diffraction patterns. This material is available free of charge via the Internet at http://pubs.acs.org.

References and Notes

(1) Motte, L.; Billoudet, F.; Pileni, M. P. *J. Phys. Chem.* **1995**, *99*, 16425.
(2) Murray, B. C.; Kagan, C. R.; Bawendi, M. G. *Science* **1995**, *270*, 1335.
(3) Pileni, M. P. *J. Phys. Chem. B* **2001**, *105*, 3358.
(4) El-Sayed, M. A. *Acc. Chem. Res.* **2001**, *34*, 257.
(5) Jin, R.; Cao, Y. C.; Hao, E.; Métraux, G. S.; Schatz, G. C.; Mirkin, C. A. *Nature* **2003**, *425*, 487.
(6) Germain, V.; Brioude, A.; Ingert, D.; Pileni, M. P. *J. Chem. Phys.* **2005**, *122*, 124707.
(7) Sanders, J. V. *Nature* **1964**, *204*, 1151.
(8) Courty, A.; Mermet, A.; Albouy, P.-A.; Duval, E.; Pileni, M. P. *Nat. Mater.* **2005**, *4*, 395.
(9) Courty, A.; Albouy, P.-A.; Mermet, A.; Duval, E.; Pileni, M. P. *J. Phys. Chem. B* **2005**, *109*, 21159.
(10) Petit, C.; Russier, V.; Pileni, M. P. *J. Phys. Chem. B* **2003**, *107*, 10333.
(11) Germain, V.; Pileni, M. P. *Adv. Mater.* **2005**, *17*, 1424.
(12) Lisiecki, I.; Parker, D.; Salzeman, C.; Pileni, M. P. *Chem. Mater.* **2007**, *19*, 4030.
(13) Ino, S.; Ogawa, S. *J. Phys. Soc. Japn.* **1967**, *22*, 1365.
(14) Allpress, J. G.; Sanders, J. V. *Surf. Sci.* **1967**, *7*, 1.
(15) Honjo, G.; Yagi, K. *J. Vac. Sci. Technol.* **1969**, *6*, 576.
(16) Yagi, K.; Takayanagi, K.; Kobayashi, K.; Honjo, G. *J. Cryst. Growth* **1975**, *28*, 117.
(17) Barkai, M.; Gruenbaum, E.; Deutscher, G. *Thin Solid Films* **1982**, *90*, 85.
(18) Heinemann, K.; Osaka, T.; Poppa, H.; Avalos-Borja, M. *J. Catal.* **1983**, *83*, 61.
(19) Doraiswamy, N.; Jayaram, G.; Marks, L. D. *Phys. Rev. B* **1995**, *51*, 10167.
(20) Baski, A. A.; Fuchs, H. *Surf. Sci.* **1994**, *313*, 275.
(21) Chapon, C.; Granjeaud, S.; Humbert, A.; Henry, C. R. *Eur. Phys. J.: Appl. Phys.* **2001**, *13*, 23.
(22) Pastoriza-Santos, I.; Liz-Marzan, L. M. *Nano Lett.* **2002**, *2*, 903.
(23) Métraux, G. S.; Mirkin, C. A. *Adv. Mater.* **2005**, *17*, 412.
(24) Jin, R.; Cao, Y. C.; Mirkin, C. A.; Kelly, K. L.; Schatz, G. C.; Zheng, J. G. *Science* **2001**, *294*, 1901.
(25) Bastys, V.; Pastoriza-Santos, I.; Rodriguez-Gonzalez, B.; Vaisnoras, R.; Liz-Marzan, L. M. *Adv. Funct. Mater.* **2006**, *16*, 766.
(26) Taleb, A.; Petit, C.; Pileni, M. P. *Chem. Mater.* **1997**, *9*, 950.
(27) Courty, A.; Lisiecki, I.; Pileni, M. P. *J. Chem. Phys.* **2002**, *116*, 8074.
(28) Motte, L.; Pileni, M. P. *Appl. Surf. Sci.* **2000**, *164*, 60.
(29) Wang, Z. L. *Adv. Mater.* **1998**, *1*, 13.
(30) Li, L.; Yang, J. J.; Minton, T. K. *J. Phys. Chem. C* **2007**, *111*, 6763.
(31) Courty, A.; Henry, A.-I.; Goubet, N.; Pileni, M. P. *Nat. Mater.* **2007**, *6*, 900.
(32) Pradeep, T.; Mitra, S.; Sreekumaran Nair, A.; Mukhopadhyay, R. *J. Phys. Chem. B* **2004**, *108*, 7012.
(33) Krost, A.; Christen, J.; Oleynik, N.; Dadgar, A.; Deiter, S.; Bläsing, J.; Krtschill, A.; Forster, D.; Bertram, F.; Diez, A. *Appl. Phys. Lett.* **2004**, *85*, 1496.
(34) Bartelt, N. C.; Theis, W.; Tromp, R. M. *Phys. Rev. B* **1996**, *54*, 11741.
(35) Peterson, M.; Zangwill, A.; Ratsch, C. *Surf. Sci.* **2003**, *536*, 55.